Internal Rotation Analysis of the Ground State Microwave Spectrum of 2-Bromopropene

E. Fliege and H. Dreizler

Abteilung Chemische Physik im Institut für Physikalische Chemie der Christian-Albrechts-Universität

Z. Naturforsch. **39 a**, 637–645 (1984); received May 21, 1984

The microwave spectrum of 2-bromopropene was reinvestigated with the use of microwave Fourier transform spectroscopy. For the two isotopic species $CH_3C^{79}Br=CH_2$ and $CH_3C^{81}Br=CH_2$ the bromine quadrupole coupling was determined with higher accuracy. The barrier hindering internal methyl rotation was obtained from the ground state.

The microwave spectrum of 2-bromopropene, $CH_3CBr=CH_2$, was initially investigated by Benz, Bauder and Günthard [1]. They assigned the spectrum in the ground and in the first excited state of the methyl torsion, and they determined the rotational and the bromine quadrupole coupling constants, and the barrier to internal rotation from the first excited torsional state.

By use of microwave Fourier transform (MWFT) spectroscopy [2, 3] it was possible to resolve the internal rotation doublets of high J lines in the ground state and to determine the hindering potential V_3.

The substance was purchased from Ega Chemie, Steinheim, with 99% purity and used after vacuum distillation.

The spectra were taken at $-60\,^\circ C$ and pressures below 1 m Torr. One of the recordings is shown in Figure 1. The lines of the ^{79}Br- and ^{81}Br-species measured in the frequency range from 8 to 18 GHz are given in Tables 1 and 2.

In order to be able to extend the measurements to higher J-values, we performed an approximate centrifugal distortion analysis with the transitions of Table I and II of [1] and our own experimental frequencies just taking the centre of the quadruplet hfs pattern of each transition. The assignment was justified by the consistency of the experimental hfs patterns with a rough first order calculation using the quadrupole coupling constants given in [1].

For our final centrifugal distortion analysis with the Hamiltonian given by Van Eijck [4] and Typke [5] we had to constrict four of the quartic constants to zero. Otherwise a singular normal equation resulted in the fitting calculations. The best fit with a standard deviation of 175 kHz for $CH_3C^{79}BR=CH_2$ and 124 kHz for $CH_3C^{81}Br=CH_2$ was obtained with the choice of δ'_J as fitting parameter besides the rotational constants. A similar observation is reported in [1]. As the centrifugal distortion analysis was used only for assignment, we did not try to improve the situation by more measurements.

The quadrupole hfs analysis was made by fitting $\chi_+ = \chi_{bb} + \chi_{cc}$ and $\chi_- = \chi_{bb} - \chi_{cc}$ to the splittings of

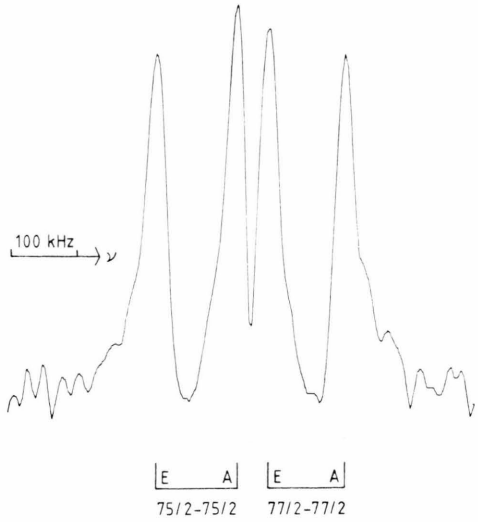

Fig. 1. A range of 700 kHz out of a 10 MHz-scan of the rotational spectrum of $CH_3C^{81}Br=CH_2$ in natural abundance. $J_{K_-K_+} - J'_{K'_-K'_+} = 38_{9,29} - 38_{9,30}$; amplitude spectrum, sample interval: 50 ns, 2048 K cycles, 1024 data points supplemented by 3072 zeros, microwave polarising frequency: $\nu_{MW} = 17449$ MHz; pressure: $p = 0.3$ mTorr, temperature: $T = -59\,^\circ C$.

Reprint requests to Prof. Dr. H. Dreizler, Institut für Physikalische Chemie der Universität Kiel, Olshausenstr. 40, D-2300 Kiel.

0340-4811 / 84 / 0700-0637 $ 01.30/0. – Please order a reprint rather than making your own copy.

Table 1. Measured transitions of $CH_3C^{79}Br{=}CH_2$. Γ: symmetry species, ν_{exp}: experimental frequency, $\bar{\nu}$: arithmetic mean of the frequencies belonging to the same hfs transition and split by internal rotation, $\bar{\nu}_0$: see text, $\bar{\nu}-\bar{\nu}_0$: measured hfs shift, $\Delta\nu_{AE}$: experimental torsional splitting, $\Delta\nu_{sim}$: corrected torsional splitting, B: measured by Benz et al. [1], *: not used for quadrupole hfs analysis, nr: not resolved; frequencies, splittings and deviations in MHz.

J	K_-	K_+	J'	K'_-	K'_+	F	F'	Γ	ν_{exp}	$\bar{\nu}-\bar{\nu}_0$	$\delta_{calc-exp}$	$\Delta\nu_{AE}$	$\Delta\nu_{sim}$	$\delta_{calc-exp}$	$\bar{\nu}_0$
2	0	2	1	0	1	7/2	5/2		10950.10	− 10.87	− 0.03	nr			10960.97
		B				5/2	5/2		11082.61	121.64	0.03				
						5/2	3/2		10948.61	− 12.36	0.02				
2	1	1	1	1	0	7/2	5/2		11757.43	− 32.43	0.00	nr			11789.86
		B				5/2	3/2		11892.09	102.23	− 0.02				
						3/2	1/2		11729.54	− 60.32	0.00				
						1/2	1/2		11658.76	− 131.10	0.01				
2	1	2	1	1	1	7/2	5/2		10233.99	− 31.66	− 0.02	nr			10265.65
		B				5/2	5/2		10296.99	31.34	− 0.03				
						5/2	3/2		10368.60	102.95	− 0.01				
						3/2	3/2		10324.76	59.11	− 0.03				
						3/2	1/2		10195.82	− 69.83	0.11				
						1/2	1/2		10134.56	− 131.09	0.00				
8	2	6	8	2	7	19/2	19/2		10325.08	− 4.47	− 0.01	nr			10329.55
		B				17/2	17/2		10335.77	6.22	0.01				
						15/2	15/2		10333.89	4.34	0.01				
						13/2	13/2		10323.03	− 6.52	0.00				
9	2	7	9	2	8			A	14606.297						14610.867
						21/2	21/2			− 4.590	− 0.013	0.040	0.039	− 0.004	
								E	14606.256						
								A	14617.065						
						19/2	19/2			6.177	0.001				
								E	14617.023						
								A	14615.384						
						17/2	17/2			4.498	0.006				
								E	14615.345						
								A	14604.435						
						15/2	15/2			− 6.451	0.009				
								E	14604.396						
11	3	8	11	3	9	25/2	25/2		7997.22	− 3.82	0.00	nr			8001.04
		B				23.2	23/2		8005.95	4.91	− 0.01				
						21/2	21/2		8004.82	3.78	0.01				
						19/2	19/2		7996.00	− 5.04	0.00				
12	3	9	12	3	10	27/2	27/2		11831.28	− 4.32	− 0.02	nr			11835.60
		B				25/2	25/2		11841.04	5.44	0.01				
						23/2	23/2		11839.89	4.29	0.01				
						21/2	21/2		11830.00	− 5.60	0.02				
13	3	10	13	3	11			A	16513.408						16518.012
						29/2	29/2			− 4.631	− 0.013	0.053	0.048	0.001	
								E	16513.353						
								A	16523.771						
						27/2	27/2			5.733	0.000				
								E	16523.718						
								A	16522.644						
						25/2	25/2			4.607	0.004				
								E	16522.593						
								A	16512.156						
						23/2	23/2			− 5.883	0.010				
								E	16512.102						
15	4	11	15	4	12	33/2	33/2		8495.52	− 3.33	− 0.01	nr			8498.85
		B				31/2	31/2		8502.89	4.04	− 0.01				
						29/2	29/2		8502.20	3.35	− 0.01				
						27/2	27/2		8494.74	− 4.11	0.01				
17	4	13	17	4	14			A	17411.767						
						37/2	37/2			− 4.362	− 0.013	0.069	0.062	0.001	
								E	17411.700						

Table 1 (continued).

J	K_-	K_+	J'	K'_-	K'_+	F	F'	Γ	ν_{exp}	$\bar{\nu}-\bar{\nu}_0$	$\delta_{calc-exp}$	$\Delta\nu_{AE}$	$\Delta\nu_{sin}$	$\delta_{calc-exp}$	$\bar{\nu}_0$
17	4	13	17	4	14										
						35/2	35/2			5.154	0.001				
								E	17421.217						
						33/2	33/2	A	17420.488	4.358	0.008				
								E	17420.420						
						31/2	31/2	A	17410.884	− 5.248	0.005				
								E	17410.811						
19	5	14	19	5	15	41/2	41/2		8515.27	− 2.86	0.00	nr			8518.13
		B				39/2	39/2		8521.44	3.31	0.01				
						37/2	37/2		8520.99	2.86	0.01				
						35/2	35/2		8514.78	− 3.35	− 0.01				
20	5	15	20	5	16										12517.533
						43/2	43/2	A	12514.100	− 3.465	− 0.013	0.064	0.057	0.001	
								E	12514.036						
						41/2	41/2	A	12521.575	4.011	0.002				
								E	12521.512						
						39/2	39/2	A	12521.045	3.480	0.006				
								E	12520.981						
						37/2	37/2	A	12513.500	− 4.065	0.005				
								E	12513.436						
21	5	16	21	5	17										17547.058
		*				45/2	45/2	A	17543.115	− 3.983	− 0.032	0.079	0.073	0.003	
								E	17543.035						
						43/2	43/2	A	17551.670	4.573	0.015				
								E	17551.592						
						41/2	41/2	A	17551.090	3.993	− 0.006				
								E	17551.011						
						39/2	39/2	A	17542.457	− 4.641	0.025				
								E	17542.377						
23	6	17	23	6	18	49/2	49/2		8210.68	− 2.40	− 0.03	nr			8213.08
		B, *				47/2	47/2		8215.79	2.71	0.03				
						45/2	45/2		8215.50	2.42	− 0.01				
						43/2	43/2		8210.31	− 2.77	0.01				
25	6	19	25	6	20										17101.718
		*				53/2	53/2	A	17098.197	− 3.566	− 0.032	0.092	0.085	0.001	
								E	17098.108						
						51/2	51/2	A	17105.779	4.014	0.016				
								E	17105.685						
						49/2	49/2	A	17105.348	3.584	− 0.004				
								E	17105.256						
						47/2	47/2	A	17097.697	− 4.067	0.020				
								E	17097.605						
28	7	21	28	7	22										11403.939
		*				59/2	59/2	A	11401.407	− 2.574	− 0.030	0.082	0.075	− 0.005	
								E	11401.324						
						57/2	57/2	A	11406.849	2.869	0.014				
								E	11406.766						

Table 1 (continued).

J	K_-	K_+	J'	K'_-	K'_+	F	F'	Γ	ν_{exp}	$\bar{\nu}-\bar{\nu}_0$	$\delta_{calc-exp}$	$\Delta\nu_{AE}$	$\Delta\nu_{sim}$	$\delta_{calc-exp}$	$\bar{\nu}_0$
28	7	21	28	7	22										
		*				55/2	55/2	A	11406.569						
										2.591	0.003				
								E	11406.490						
						53/2	53/2	A	11401.074						
										− 2.907	0.014				
								E	11400.991						
29	7	22	29	7	23										16240.608
		*				61/2	61/2	A	16237.517						
										− 3.141	− 0.034	0.098	0.095	− 0.002	
								E	16237.418						
						59/2	59/2	A	16244.143						
										3.487	0.017				
								E	16244.046						
						57/2	57/2	A	16243.820						
										3.163	0.001				
								E	16243.722						
						55/2	55/2	A	16237.125						
										− 3.531	0.016				
								E	16237.029						
32	8	24	32	8	25										10514.005
		*				67/2	67/2	A	10511.873						
										− 2.176	− 0.033	0.083	0.076	− 0.004	
								E	10511.786						
						65/2	65/2	A	10516.445						
										2.400	0.016				
								E	10516.365						
						63/2	63/2	A	10516.246						
										2.198	0.004				
								E	10516.159						
						61/2	61/2	A	10511.609						
										− 2.435	0.013				
								E	10511.531						
33	8	25	33	8	26										15100.102
		*				69/2	69/2	A	15097.426						
										− 2.727	− 0.038	0.101	0.097	0.000	
								E	15097.325						
						67/2	67/2	A	15103.148						
										2.995	0.021				
								E	15103.046						
						65/2	65/2	A	15102.903						
										2.751	0.006				
								E	15102.803						
						63/2	63/2	A	15097.117						
										− 3.035	0.011				
								E	15097.017						
36	9	27	36	9	28										9527.905
		*				75/2	75/2	A	9526.128						
										− 1.817	− 0.038	0.076	0.069	0.003	
								E	9526.049						
						73/2	73/2	A	9529.932						
										1.990	0.020				
								E	9529.858						
						71/2	71/2	A	9529.788						
										1.847	0.004				
								E	9529.715						
						69/2	69/2	A	9525.914						
										− 2.030	0.016				
								E	9525.836						
37	9	28	37	9	29										13793.844
		*				75/2	75/2	A	13796.454						
										2.560	0.011	0.100	0.096	0.002	
								E	13796.354						
						73/2	73/2	A	13796.277						
										2.383	− 0.010				
								E	13796.177						

Table 2. Measured transitions of $CH_3C^{81}Br=CH_2$. Γ: symmetry species, ν_{exp}: experimental frequency, $\bar{\nu}$: arithmetic mean of the frequencies belonging to the same hfs transition and split by internal rotation, $\bar{\nu}_0$: see text, $\bar{\nu}-\bar{\nu}_0$: measured hfs shift, $\Delta\nu_{AE}$: experimental torsional splitting, $\Delta\nu_{sim}$: corrected torsional splitting, B: measured by Benz et al. [1], *: not used for quadrupole hfs analysis, nr: not resolved; frequencies, splittings and deviations in MHz.

J	K_-	K_+	J'	K'_-	K'_+	F	F'	Γ	ν_{exp}	$\bar{\nu}-\bar{\nu}_0$	$\delta_{calc-exp}$	$\Delta\nu_{AE}$	$\Delta\nu_{sim}$	$\delta_{calc-exp}$	$\bar{\nu}_0$
2	0	2	1	0	1	7/2	5/2		10874.69	− 9.16	0.01	nr			10883.85
		B				5/2	3/2		10873.57	− 10.28	− 0.01				
2	1	1	1	1	0	7/2	5/2		11672.92	− 27.14	− 0.01	nr			11700.06
		B				5/2	5/2		11733.26	33.20	− 0.05				
						5/2	3/2		11785.26	85.20	0.02				
						3/2	3/2		11742.69	42.63	− 0.03				
						3/2	1/2		11649.30	− 50.76	0.06				
2	1	2	1	1	1	7/2	5/2		10170.63	− 26.53	0.01	nr			10197.16
		B				5/2	5/2		10223.25	26.09	− 0.04				
						5/2	3/2		10282.99	85.83	0.00				
						3/2	3/2		10246.21	49.05	0.03				
						1/2	1/2		10087.28	− 109.88	0.00				
9	2	7	9	2	8			A	14282.713						14286.509
						21/2	21/2			− 3.813	0.021	0.035	0.034	0.000	
								E	14282.679						
								A	14291.660						
						19/2	19/2			5.133	− 0.048				
								E	14291.624						
								A	14290.259						
						17/2	17/2			3.732	− 0.031				
								E	14290.222						
								A	14281.175						
						15/2	15/2			− 5.350	0.059				
								E	14281.142						
13	3	10	13	3	11			A	15993.439						15997.233
						29/2	29/2			− 3.821	0.016	0.052	0.047	0.001	
								E	15993.385						
								A	16001.988						
						27/2	27/2			4.730	− 0.035				
								E	16001.937						
								A	16001.055						
						25/2	25/2			3.796	− 0.025				
								E	16001.002						
								A	15992.414						
						23/2	23/2			− 4.844	0.043				
								E	15992.364						
16	4	12	16	4	13			A	11912.660						11915.804
						35/2	35/2			− 3.170	− 0.011	0.054	0.048	− 0.001	
								E	11912.608						
								A	11911.974						
						29/2	29/2			− 3.857	0.011				
								E	11911.919						
17	4	13	17	4	14			A	16684.932						16688.466
						37/2	37/2			− 3.567	0.009	0.067	0.060	0.001	
								E	16684.866						
								A	16692.719						
						35/2	35/2			4.220	− 0.028				
								E	16692.653						
								A	16692.062						
						33/2	33/2			3.564	− 0.018				
								E	16691.997						
								A	16684.209						
						31/2	31/2			− 4.292	0.035				
								E	16684.139						
20	5	15	20	5	16			A	11792.806						11795.549
						43/2	43/2			− 2.780	0.000	0.072	0.065	− 0.010	
								E	11792.731						

Table 2 (continued).

J	K_-	K_+	J'	K'_-	K'_+	F	F'	Γ	ν_{exp}	$\bar{\nu}-\bar{\nu}_0$	$\delta_{calc-exp}$	$\Delta\nu_{AE}$	$\Delta\nu_{sim}$	$\delta_{calc-exp}$	$\bar{\nu}_0$
20	5	15	20	5	16										
						41/2	41/2	A	11798.810						
										3.226	−0.019				
								E	11798.739						
						39/2	39/2	A	11798.372						
										2.788	−0.005				
								E	11798.302						
						37/2	37/2	A	11792.318						
										−3.267	0.025				
								E	11792.246						
21	5	16	21	5	17										16618.549
		*				45/2	45/2	A	16615.360						
										−3.227	−0.007	0.077	0.070	0.002	
								E	16615.284						
						43/2	43/2	A	16622.297						
										3.709	−0.013				
								E	16622.219						
						41/2	41/2	A	16621.819						
										3.231	−0.020				
								E	16621.741						
						39/2	39/2	A	16614.827						
										−3.761	0.042				
								E	16614.750						
24	6	18	24	6	19										11258.655
		*				49/2	49/2	A	11261.388						
										2.700	−0.004	0.067	0.060	0.001	
								E	11261.322						
						47/2	47/2	A	11261.086						
										2.398	−0.014				
								E	11261.019						
25	6	19	25	6	20										15992.953
		*				53/2	53/2	A	15990.149						
										−2.847	−0.020	0.086	0.079	0.002	
								E	15990.063						
						51/2	51/2	A	15996.226						
										3.230	−0.019				
								E	15996.140						
						49/2	49/2	A	15995.875						
										2.879	−0.026				
								E	15995.789						
						47/2	47/2	A	15989.746						
										−3.250	0.025				
								E	15989.661						
28	7	21	28	7	22										10454.560
		*				59/2	59/2	A	10452.580						
										−2.016	−0.012	0.070	0.063	0.002	
								E	10452.509						
						57/2	57/2	A	10456.838						
										2.245	0.000				
								E	10456.772						
						55/2	55/2	A	10456.624						
										2.028	−0.008				
								E	10456.552						
						53/2	53/2	A	10452.321						
										−2.274	0.021				
								E	10452.251						
29	7	22	29	7	23										14983.844
		*				61/2	61/2	A	14981.404						
										−2.486	−0.013	0.092	0.085	0.002	
								E	14981.313						
						59/2	59/2	A	14986.652						
										2.762	−0.004				
								E	14986.560						
						57/2	57/2	A	14986.388						
										2.499	−0.009				
								E	14986.297						
						55/2	55/2	A	14981.096						
										−2.795	0.028				
								E	14981.002						

Table 2 (continued).

J	K_-	K_+	J'	K'_-	K'_+	F	F'	Γ	ν_{exp}	$\bar{\nu}-\bar{\nu}_0$	$\delta_{calc-exp}$	$\Delta\nu_{AE}$	$\Delta\nu_{sim}$	$\delta_{calc-exp}$	$\bar{\nu}_0$
32	8	24	32	8	25										9499.658
		*				67/2	67/2	A	9498.014						
								E	9497.945	−1.679	−0.016	0.071	0.064	0.002	
						65/2	65/2	A	9501.544						
								E	9501.473	1.851	0.003				
						63/2	63/2	A	9501.389						
								E	9501.316	1.695	−0.005				
						61/2	61/2	A	9497.817						
								E	9497.746	−1.877	0.018				
33	8	25	33	8	26										13735.088
		*				69/2	69/2	A	13733.007						
								E	13732.915	−2.127	−0.019	0.093	0.086	0.003	
						67/2	67/2	A	13737.475						
								E	13737.381	2.340	0.001				
						65/2	65/2	A	13737.279						
								E	13737.186	2.145	−0.005				
						63/2	63/2	A	13732.764						
								E	13732.670	−2.371	0.024				
36	9	27	36	9	28										8481.742
		*				75/2	75/2	A	8480.399						
								E	8480.330	−1.378	−0.025	0.068	0.061	0.003	
						73/2	73/2	A	8483.285						
								E	8483.218	1.510	0.009				
						71/2	71/2	A	8483.179						
								E	8483.112	1.404	−0.005				
						69/2	69/2	A	8480.234						
								E	8480.165	−1.543	0.020				
37	9	28	37	9	29										12363.437
		*				77/2	77/2	A	12361.702						
								E	12361.601	−1.786	−0.033	0.104	0.100	−0.011	
						75/2	75/2	A	12365.448						
								E	12365.340	1.957	0.009				
						73/2	73/2	A	12365.302						
								E	12365.200	1.814	0.001				
						71/2	71/2	A	12361.493						
								E	12361.390	−1.996	0.025				
38	9	29	38	9	30										17445.120
		*				79/2	79/2	A	17442.959						
								E	17442.840	−2.221	−0.033	0.119	0.114	0.003	
						77/2	77/2	A	17447.599						
								E	17447.484	2.422	0.010				
						75/2	75/2	A	17447.436						
								E	17447.316	2.256	−0.006				
						73/2	73/2	A	17442.716						
								E	17442.595	−2.465	0.028				

Table 3. Rotational [MHz], centrifugal distortion [kHz] and bromine-hfs [MHz] constants of 2-bromopropene. N: number of lines, σ: standard deviation of the fit [kHz], $\overline{\Delta\nu_{exp}}$: mean experimental hfs splitting [MHz]; standard errors in units of the last digit in brackets. The centrifugal distortion constants D'_J, D'_{JK}, D'_K and R'_6 were assumed to be zero.

	$CH_3C^{79}Br=CH_2$	Correlation matrix				$CH_3C^{81}Br=CH_2$	Correlation matrix			
A	9256.00 (10)	1.00				9255.942 (78)	1.00			
B	3138.011 (26)	0.38	1.00			3112.878 (18)	0.38	1.00		
C	2375.879 (26)	0.11	0.96	1.00		2361.434 (18)	0.08	0.95	1.00	
δ'_J	0.14557 (71)	− 0.83	− 0.10	0.10	1.00	0.14304 (43)	− 0.81	− 0.11	0.11	1.00
N	21					18				
σ	175					124				
χ_+	− 534.474 (53)	1.000				− 446.653 (71)	1.000			
χ_-	− 38.222 (59)	0.040	1.000			− 31.546 (89)	0.008	1.000		
N	12					8				
σ	29					36				
$\overline{\Delta\nu_{exp}}$	26.591					29.760				
χ_{aa}	534.474 (53)					446.653 (71)				
χ_{bb}	− 286.348 (56)					− 239.100 (80)				
χ_{cc}	− 248.126 (56)					− 207.554 (80)				

Table 4. Internal rotation parameters of 2-bromopropene. $w_1(s)$: Fourier coefficient, $\sphericalangle(a, i)$, $\sphericalangle(b, i)$: angle between the inertia axis a resp. b and the internal rotation axis i, I_α: moment of inertia of the methyl group, N: number of lines, $|(a, b)|$: correlation between a and b, σ: standard deviation of the fit, $\overline{\Delta\nu_{AE}}$: mean experimental torsional splitting, s: reduced barrier height, V_3: barrier to internal rotation, F: reduced rotational constant of the internal rotation, λ_a, λ_b: direction cosines of $\sphericalangle(a, i)$ and $\sphericalangle(b, i)$; standard errors in units of the last digit in brackets, fixed values in square brackets, derived parameters below the line.

	$CH_3C^{79}Br=CH_2$	$CH_3C^{81}Br=CH_2$
$w_1(s)$	$-4.13\,(69\cdot10^{-6})$	$-4.3\,(11)\cdot10^{-6}$
$\sphericalangle(a, i)$ [°]	57.8 (34)	56.9 (48)
I_α [amuÅ^2]	[3.167]	[3.167]
N	12	15
$\lvert(w_1(s), \sphericalangle(a, i))\rvert$	0.998	0.998
σ [kHz]	3	5
$\overline{\Delta\nu_{AE}}$ [kHz]	73	69
s	72.8 (14)	72.4 (21)
V_3 [cal/mol]	2571 (49)	2558 (74)
F [GHz]	164.64	164.72
$\sphericalangle(b, i)$ [°]	32.2 (34)	33.1 (48)
λ_a	0.533 (51)	0.546 (72)
λ_b	0.846 (30)	0.838 (43)

lines up to $J = 20$ with a program diagonalising the Hamiltonian matrix [6]. Lines with higher J-values could not be included into the fit because of computer time and core capacity. The off-diagonal tensor element χ_{ab} could not be determined, since the measured lines are not sensitive enough to this parameter. We did not follow the χ_{ab} variation procedure reported in [1].

The line centres $\bar{\nu}_0$ of the hfs patterns were calculated by first averaging the internal rotation splittings (frequencies $\bar{\nu}$) and by secondly applying the hfs shifts predicted for lines up to $J = 20$ by means of direct diagonalisation and for higher J-values according to first order theory with the constants of Table 3. These frequencies $\bar{\nu}_0$ were the input for the centrifugal distortion analysis.

The results of the bromine quadrupole hfs and the centrifugal distortion analysis are given in Table 3.

For the internal rotation analysis we took the mean internal rotation splitting of the hfs components for each rotational line. This is equivalent to the approximation that nuclear quadrupole coupling and internal rotation do not interact.

As we noticed [7] that the spacings of narrowly split lines by the power spectra of MWFT are displayed slightly too large, we corrected the frequencies. From many line shape analyses of $CH_3C^{35}Cl=CH_2$ and $CH_3C^{79}Br=CH_2$ we got the same empirical dependence of the correction as a function of the splitting. This empirical correction was also applied to $CH_3C^{81}Br=CH_2$. The corrected splittings ($\Delta\nu_{sim}$ of Tables 1 and 2) are the basis for the internal rotation analysis.

The analysis was performed by the internal axis method (IAM) with a program by Woods [8, 9] which was modified [10, 11]*. The rotational constants of Table 3 were used. An attempt to fit the potential parameter $w_1(s)$, the angle $\sphericalangle(a, i)$ be-

* Programs DDIRFI, FIDIC, and F05MOD.

Table 5. Comparison of potential barriers V_3 of 2-halopropenes $CH_3CX=CH_2$. $I_\alpha = 3.167$ amuÅ^2 was assumed [12]. Further assumption in square brackets, standard deviations in brackets.

X	F	^{35}Cl	^{37}Cl	^{79}Br	^{81}Br
V_3 [cal/mol]	2407.3 (37)	2568 (10)	2582 (12)	2571 (49)	2558 (74)
$\measuredangle$ (a, i) [°]	[3.03]	59.78 (84)	61.28 (108)	57.8 (34)	56.9 (48)
F [GHz]	170.43	165.91	165.69	164.64	164.72
s	65.84 (10)	72.15 (29)	72.63 (35)	72.8 (14)	72.4 (21)

tween the a- and the internal rotation axis and the moment of inertia I_α of the methyl group resulted in an unreasonably high $I_\alpha = 3.32$ amuÅ^2 and $I_\alpha = 3.69$ amuÅ^2 for the ^{79}Br- and ^{81}Br-species. So we decided to assume $I_\alpha = 3.167$ amuÅ^2 like in the analysis of 2-chloropropene [12].

The results of the internal rotation analysis are given in Table 4. It should be mentioned that the barriers V_3 and the angles $\measuredangle$ (a, i) of both isotopes coincide within the error limits.

To check the values of the angle $\measuredangle$ (a, i), we performed tentative r_0-structure calculations. Unfortunately the information by the known six rotational constants is limited. So we transferred the structural data of 2-chloropropene of Tab. V of [13] and fitted the bond length $\overline{CBr}$ and the angle $\measuredangle$ CCBr. The angle of an internal rotation axis perpendicular to the plane of the three methyl hydrogen atoms with respect to the a-axis is roughly 62° for both isotopes. Considering the inherent errors the agreement is satisfactory.

We also repeated the internal rotation analyses for 2-chloropropene $CH_3C^xCl=CH_2$ with $x = 35$ and 37 using corrected torsional splittings $\Delta\nu_{sim}$. The values of Table 5 of [12] thereupon only change within the error limits.

Presently the methyl torsion analyses of the 2-halopropenes $CH_3CX=CH_2$ with X = F [14], ^{35}Cl, ^{37}Cl [12], ^{79}Br, and ^{81}Br [this paper] are available. As the PAM-analysis for $CH_3CF=CH_2$ given in Table 5 of [14] is based on $I_\alpha = 3.11$ amuÅ^2 which was taken from propylene, we repeated for comparison the analysis with $I_\alpha = 3.167$ amuÅ^2 and $\measuredangle$ (a, i) = 3.03° *. Without the assumption of $\measuredangle$ (a, i) from the structure Fig. 1 of [14] the fit diverged. The result is given in Table 5. With more precise measurements as they are possible nowadays, the torsional analysis for 2-fluoropropene could most probably be improved.

There is a substantial difference of the V_3-values between the fluorine and the other halogen compounds. This has already been stated in [1], but the values of Table 5 stem all from an analysis of the ground state torsional fine structure carried out by the same method (IAM) under equivalent assumptions.

We thank the members of our group and especially Dipl.-Phys. G. Bestmann for help and the Deutsche Forschungsgemeinschaft and Fond der Chemie for funds.

* The line $28_{20,8} - 28_{20,9}$ was omitted.

[1] H. P. Benz, A. Bauder, and Hs. H. Günthard, J. Mol. Spectr. **21,** 165 (1966).
[2] G. Bestmann, H. Dreizler, H. Mäder, and U. Andresen, Z. Naturforsch. **35 a,** 392 (1980).
[3] G. Bestmann and H. Dreizler, Z. Naturforsch. **37 a,** 58 (1982).
[4] B. P. van Eijck, J. Mol. Spectr. **53,** 246 (1974).
[5] V. Typke, J. Mol. Spectr. **63,** 170 (1976); program ZFAP4 by V. Typke (1982).
[6] D. Hübner and M. Stolze, programs NQ20A and NQ20S, diplom theses, Kiel 1980.
[7] E. Fliege and H. Dreizler, Z. Naturforsch. **39 a,** (1984).
[8] R. C. Woods, J. Mol. Spectr. **21,** 4 (1966).
[9] R. C. Woods, J. Mol. Spectr. **22,** 49 (1967).
[10] J. Meier, Dissertation 4611, ETH Zurich 1970.
[11] Modified by H. Lutz and E. Fliege, Kiel.
[12] E. Fliege and H. Dreizler, Z. Naturforsch. **38 a,** 1231 (1983).
[13] W. Good, R. J. Conan, jr., A. Bauder, and Hs. H. Günthard, J. Mol. Spectr. **41,** 381 (1972).
[14] L. Pierce and J. M. O'Reilly, J. Mol. Spectr. **3,** 536 (1959).